Verification and Validation of the Foredrag Coefficient for Supersonic and Hypersonic Flow of Air Over Cones

Guilherme Bertoldo
UTFPR - Universidade Tecnológica Federal do Paraná,
Câmpus Francisco Beltrão,
85601-970, Francisco Beltrão, PR,
E-mail: gbertoldo@utfpr.edu.br,

Carlos Henrique Marchi,
UFPR - Departamento de Engenharia Mecânica,
Câmpus Politécnico,
81531-970, Curitiba, PR,
E-mail: marchi@ufpr.br

Abstract: *The foredrag coefficient due to the supersonic and hypersonic flow of air over cones was calculated numerically using a finite volume approach based on the compressible Euler and Navier-Stokes equation with constant thermophysical properties. Simulations were carried on for a cone of* 10° *semi-angle under the free-stream Mach numbers* $M_\infty = 2$*, 3, 4, 5, 6 and 8 in the case of Euler model and for a cone of fineness ratio 3 under the free-stream Mach numbers 2.73, 3.50, 4.00, 5.05 and 6.28 in the case of Navier-Stokes model (the Reynolds number, based on the cone length, are within* 4.5×10^5 *and* 2.85×10^6*). The numerical error was estimated to be lower than* 0.08% *of the numerical solution for both models. Comparison of the solution of the Navier-Stokes model with the experimental data of Eggers et al.[3], showed a disagreement up to* 0.88% *for* $2.73 \leq M_\infty < 6.28$ *and of* 15% *for* $M_\infty = 6.28$*. The validation uncertainty was estimated to be, at most,* 7.2%*.*

Keywords: *CFD, Verification, Validation, Cone, Supersonic, Hypersonic*

1 Introduction

In Computational Fluid Dynamics (CFD), a software may be considered a more reliable tool for flow prediction after their results have been verified and validated. According to Roache[9], verification estimates the error caused by solving approximately a mathematical model, while validation estimates the error caused by the modeling itself. Taking into account the importance of error estimation in scientific computing, this work deals with verification and validation of the foredrag coefficient calculated by the Mach2D code, a software that is under development by the CFD group at Federal University of Paraná and solves the compressible Euler and Navier-Stokes equations based on a finite volume approach.

The foredrag coefficient considered here is due to the axisymmetric air flow over cones calculated for some values of the Mach number in the supersonic and hypersonic regimes. More precisely, the simulations are separated in two sets. In the first one, the foredrag coefficient is calculated based on the Euler equations for a cone of 10° semi-angle and under the free-stream Mach numbers 2, 3, 4, 5, 6 and 8. In the second set, the foredrag coefficient is calculated based on the laminar Navier-Stokes equations for a cone of fineness ratio $f = 3$ (length/base diameter) and under the free-stream Mach numbers 2.73, 3.50, 4.00, 5.05 and 6.28. These cone geometries and Mach numbers were chosen because of available data (numerical and experimental) of other authors that are used in the comparisons.

The verification and validation procedures are applied for the foredrag of the Navier-Stokes model, while the foredrag of the Euler model is only verified. The applied procedures are based on the recommendations of ASME V&V 20-2009 norm[1].

This work has two purposes First it aims to evaluate the results produced by the Mach2D code using verification and validation tools and, second, to register the obtained results in tables, so that other CFD software developers may compare their results with the results presented here. Based on the authors

experience, it is very difficult to find tabulated CFD results for comparisons in the open literature, even for simple geometries as the conical one.

In the next sections, the method of foredrag calculation, the verification and validation procedures and the main results are presented.

2 Methodology

2.1 Flow simulation

The flow is modeled by the time dependent compressible Navier-Stokes equation for axisymmetric flows[2]. The thermophysical properties, *i.e.*, viscosity, thermal conductivity and specific heats, are considered constant and equal to their free-stream values. For each gas specie, the thermophysical properties are calculated according to the interpolation formulas of McBride *et al.*[7] as a function of the free-stream temperature T_∞ and for a gas mixture according to Refs. [2] and [13]. In this study, the air is a mixture of Ar, O_2 and N_2 in the molar fractions of 1%, 21% and 78%, respectively. The Euler model is obtained neglecting all terms depending on the viscosity and thermal conductivity. The ideal gas state equation is used for the coupling among pressure p, density ρ and temperature T. The domain of calculation, Fig 1(a), is simplified due to the axial symmetry Over the north boundary N (a quarter of ellipse), the flow is non-perturbed and equal to the free-stream, where the Mach number M_∞, Reynolds Re_∞ (based on the cone length l_r) and temperature T_∞ are prescribed. On the west boundary W, the symmetry conditions are applied. Over the south boundary S, the normal pressure and temperature gradient is zero, while the non-slip condition is applied to the velocity field in the case o Navier-Stokes model and the non-permeability condition is applied to the Euler model. Finally, the outflow is considered locally parabolic over the east boundary E.

In order to simplify the numerical solution, the governing equations are transformed[5] from the cylindrical coordinate system (x, y) to a curvilinear coordinate system (ξ, η), in such a way that the physical domain is mapped into a rectangular domain (computational domain). The physical domain is algebraically discretized with nodes concentrated near the cone surface and the cone tip (Fig. 1(b)). The x coordinate of the south and north boundaries (η lines) is discretized according to a power law distribution with exponent α. The lines connecting the north and south boundaries (ξ lines) are discretized in such a way that the partition widths form a geometric progression. The width of the partition close to the cone surface is a multiple c_{bl} of the estimated boundary layer width δ, which is given by

$$\delta = \sqrt{\frac{\mu_\infty l_r}{\rho_\infty u_\infty}}, \tag{1}$$

where μ_∞, ρ_∞ and u_∞ are, respectively, the free-stream viscosity, density and speed. The transformed Navier-Stokes equations are then integrated on each volume of the uniformly discretized computational domain using a co-located grid arrangement. The variables over the volumes faces are interpolated from the center of each volume in the computational domain using a first order accurate scheme (upstream differencing scheme) for the advective terms and a second order accurate scheme (central differencing scheme) for the diffusive terms[16]. After that, four systems of coupled linearized equations are obtained representing the mass, momentum (x and y components) and energy conservation. The discretized mass equation is transformed in an equation for the pressure correction based on the SIMPLEC algorithm[15]. The pressure correction equation takes into account the influence of the compressibility as well as the pressure-velocity coupling in the same way as did Ferziger and Peric[4]. Each of the linear systems is solved with the *Modified Strongly Implicit* method (MSI)[14]. The set of coupled linear systems are solved iteratively following a false transient until the stationary solution is obtained.

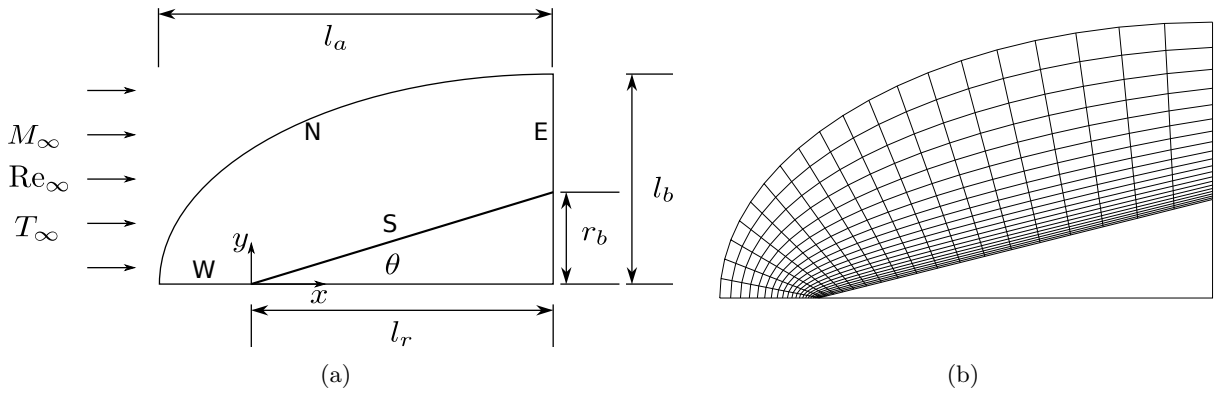

Figure 1: Schematic illustration of the (a) domain of calculation and (b) its discretization.

2.2 Verification

In CFD, there are basically four sources of numerical errors[6]: (i) coding mistakes, (ii) round-off errors (iii) iteration errors and (iv) truncation errors. The combination of each of these errors gives the overall numerical error.

The coding mistakes errors are difficult to identify and are caused by programming errors or mistakes in the software usage. In order to avoid them, some strategies were applied. First, the Mach2D code was completely rewritten from an older version. The code development was tracked by the *Subversion* version control system[8]. During this task and after typing each subroutine, the numerical solution was compared to the numerical solution of the original code. Second, the code was compiled with two compilers (GNU Fortran Compiler-*v.*4.8.2 and Intel Fortran Compiler-*v.*13.1.1) using their debug directives. And third, memory check was performed with the *Valgrind* tool[11]. Based on this procedure, one hopes that the Mach2D code, more precisely Mach2D-5.8.2.2-r528, is free from coding mistakes.

Round-off errors are caused by the limited representation of real numbers. Its influence on the solution may be estimated, for instance, comparing the solution obtained with double precision floating point representation (16 significant figures) with the solution obtained with quadruple precision floating point representation (32 significant figures). In this comparison, it is assumed that the round-off error in the quadruple precision solution is vanishingly small compared to the double precision one. The change in the precision of the representation is easily made with the GNU Fortran Compiler through the directive *-freal-8-real-16*, which converts double precision variables to quadruple precision ones.

Iteration error is, by definition, the difference between the numerical solution at some iteration and the exact numerical solution of the discretized model. In this work, the iterations are performed until the machine error is reached, so that the iteration errors may be considered negligibly small.

Finally, the truncation error results from the approximations related to the discretization of the mathematical model. This is typically the greatest source of the numerical error. When the numerical error is dominated by the truncation error, the former is called discretization error[6].

In this study, the discretization error was calculated with the convergent estimator[6]. In order to perform this calculation, consider that three numerical solutions, ϕ_1, ϕ_2 and ϕ_3 were obtained in grids with uniform partitions h_1, h_2 and h_3, respectively, and that the grid refinement ratio r is a constant, *i.e.*,

$$r = \frac{h_2}{h_1} = \frac{h_3}{h_2} > 1. \tag{2}$$

According to the convergent estimator, the exact solution Φ of the mathematical model is given by the convergent estimation of the analytical solution ϕ_C and its estimated error U_C as

$$\Phi = \phi_C \pm U_C, \tag{3}$$

where

$$\phi_C = \frac{\phi_{\mathrm{Ri}}(p_L) + \phi_{\mathrm{Ri}}(p_U)}{2} \tag{4}$$

and

$$U_C = \frac{|\phi_{\mathrm{Ri}}(p_L) - \phi_{\mathrm{Ri}}(p_U)|}{2}. \tag{5}$$

In Eqs. (4) and (5), ϕ_{Ri} is the Richardson extrapolation of the numerical solutions based on the asymptotic order of accuracy p_L or based on the observed order of accuracy p_U. The asymptotic order of accuracy p_L is the dominant order of accuracy obtained from the truncation error for a sufficiently refined grid (first order accurate in this study, *i.e.*, $p_L = 1$) and the observed order p_U is calculated from

$$p_U = \frac{\log\left(\frac{\phi_2 - \phi_3}{\phi_1 - \phi_2}\right)}{\log r}. \tag{6}$$

The Richardson extrapolation for an arbitrary order of accuracy p_A, and based on the finest grid h_1, is given by

$$\phi_{\mathrm{Ri}}(p_A) = \phi_1 + \frac{\phi_1 - \phi_2}{r^{p_A} - 1}. \tag{7}$$

Theoretically, the exact solution Φ of the mathematical model is bounded by the convergent estimation and its error estimative. However, the application of this estimator requires that the observed order p_U is within the convergent range, *i.e.*, that p_U decreases or increases monotonically toward p_L as the grid is refined.

2.3 Validation

According to the ASME V&V 20-2009 norm[1], the error in a simulation result ϕ^{num} due to modeling assumptions and approximations δ^{model} is expected to be within the interval

$$E - U^{\mathrm{val}} \leq \delta^{\mathrm{model}} \leq E + U^{\mathrm{val}}, \tag{8}$$

where E and U^{val} are the validation metrics. E is given by

$$E = \phi^{\mathrm{num}} - \phi^{\mathrm{exp}} \tag{9}$$

and U^{val} depends on how the experimental result ϕ^{exp} was obtained. For the case in which ϕ^{exp} is directly measured, U^{val} reads

$$U^{\mathrm{val}} = \sqrt{(U^{\mathrm{num}})^2 + (U^{\mathrm{input}})^2 + (U^{\mathrm{exp}})^2}, \tag{10}$$

where U^{num} is the estimate of the numerical error, whose method of calculation was presented in the previous section, U^{input} is the estimate of the uncertainty in the numerical solution caused by the variability of the input parameters and U^{exp} is the estimate of the uncertainty in the experimental measurement. Considering the existence of n input parameters X_i ($1 \leq i \leq n$), U^{input} is calculated as

$$(U^{\mathrm{input}})^2 = \sum_1^n \left(\frac{\partial \phi^{\mathrm{num}}}{\partial X_i} U_{X_i}\right)^2, \tag{11}$$

where U_{X_i} is the standard uncertainty in X_i.

In this work, ϕ^{exp} represents the foredrag coefficient C_{Df} from the experiment of Eggers *et al.*[3]. The foredrag coefficient was not directly measured, but obtained from a data reduction involving some data that are input parameters for the mathematical model. Because of that, Eq. (10) is not the appropriate expression to U^{val}. The appropriate expression, however, involves experimental data that are not available So, Eq. (10) will be used at least as an approximation to U^{val}.

3 Results and Discussion

3.1 Euler model

This section deals with the verification of the pressure foredrag C_{Df}^{p} of the Euler model, which was carried on for six values of the Mach number: 2, 3, 4, 5, 6 and 8. The input parameters used in the simulations are shown in Tab. 1. For each Mach number, simulations were performed on five grids m_5, m_4, m_3, m_2 and m_1 with, respectively, 60, 120, 240, 480 and 960 volumes in each coordinate direction. The coarser grids were obtained from the finest one by removing every other grid line.

Table 1: Input data for the Euler model.

Quantity	Symbol	Value
Free stream pressure	p_∞	300 Pa
Free stream temperature	T_∞	300 K
Length of the elliptical x semi-axis	l_a	3.1 m
Length of the elliptical y semi-axis ($M = 2$)	l_b	2.5 m
Length of the elliptical y semi-axis ($M > 2$)	l_b	1.5 m
Base radius	r_b	0.5 m
Cone semi-angle	θ	10°
Exponent for boundary nodes distribution	α	2
Multiple of the estimated boundary layer width	c_{bl}	0.05

In order to investigate the effect of the round-off error, C_{Df}^{p} was calculated using double and quadruple precision. This test was limited to a specific simulation (mesh of 960×960 volumes and $M_\infty = 2$) due to the computational expense of the quadruple precision simulation. Figure 2 shows the behavior of the relative round-off error of C_{Df}^{p} as a function of the number of iterations. As can be seen, this error reach an expressive value (more than 10^{-8}) during the false transient, but becomes lower than 10^{-14} for the converged solution.

Figure 2 also shows the behavior of the residuals of the linear systems and the residual of the mass conservation equation as a function of the number of iterations for the same particular simulation. The residual of the linear systems reaches the machine zero at about 9000 iterations, but the iteration procedure is kept until about 17000 iterations in order to ensure that the iteration errors are vanishingly small. This behavior was observed in all the simulations.

Based on these results, the authors believe that both the iterative error and the round-off error are negligibly small compared to the truncation error, which allows one to proceed with the calculation of the numerical error following the methodology described in Sec. 2.2.

Looking for the estimation of the discretization error, the observed order of accuracy p_U was obtained with the five grids above mentioned. The results are shown in Tab. 2 for the six Mach numbers under consideration One can see that the observed order approximates the asymptotic order as the grid is refined, that is, $p_U \to p_L = 1$. This fact has two positive aspects: (i) the convergent estimator can be applied and (ii) according to Roy[10], the convergence of the observed order p_U to the asymptotic one p_L should be verified when the code is free from coding mistake errors.

The foredrag coefficient estimated with the convergent estimator is presented in the first row of Tab. 3. The values in the parenthesis represent the estimated error. For instance, 0.104 47(3) means $0.104\,47 \pm 0.000\,03$. The estimated numerical error do not exceed 0.06% of the estimated solution for the whole interval of Mach numbers considered.

Table 3 also shows the solutions obtained with different grid clustering. As mentioned earlier, α controls the clustering near the tip, while c_{bl} controls the clustering near the body surface. In order to investigate the grid clustering influence on the final solution, it was considered a grid with less concentration of points near the tip ($\alpha = 1.5$) and a grid with more concentration ($\alpha = 2.5$). The same was

Figure 2: Residual of the linear systems, residual of the mass conservation equation and round-off relative error of C_{Df}^{p}. Euler model. Mesh: 960×960. $M_\infty = 2$.

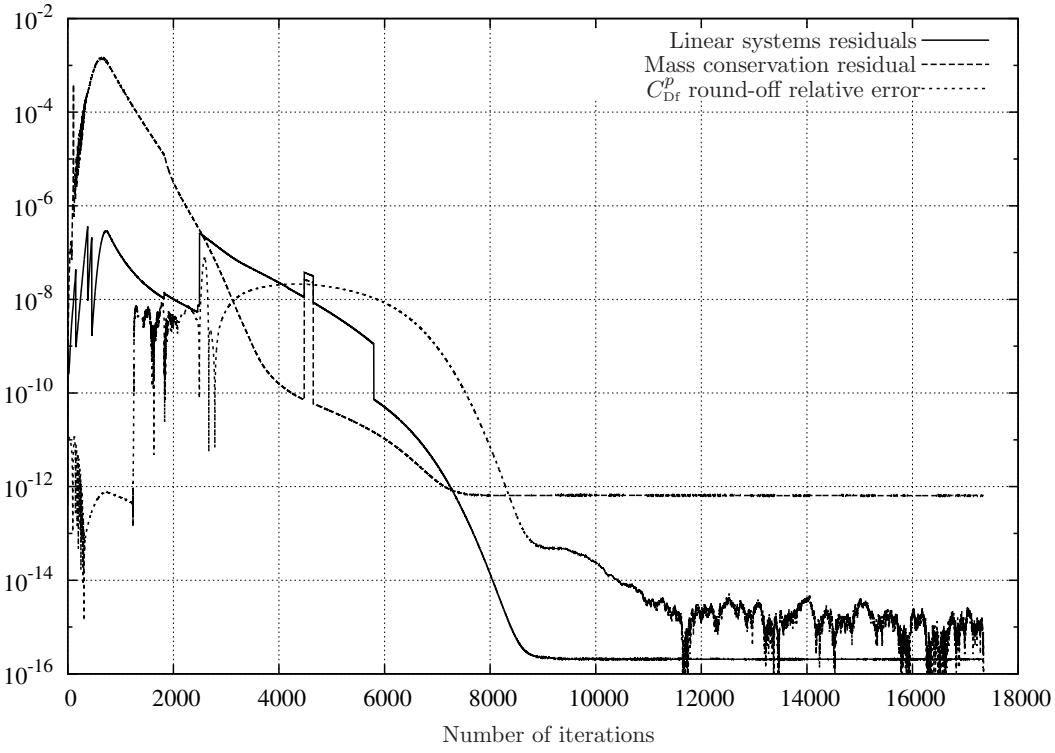

Table 2: Observed order of accuracy p_U for the pressure foredrag C_{Df}^{p} calculated for several Mach numbers. Euler model.

	p_U					
Meshes	$M_\infty = 2$	3	4	5	6	8
(m_3, m_4, m_5)	0.46	0.64	0.65	0.70	0.76	0.85
(m_2, m_3, m_4)	0.67	0.72	0.75	0.81	0.86	0.92
(m_1, m_2, m_3)	0.75	0.76	0.82	0.88	0.92	0.96

done to the concentration near the body surface ($c_{bl} = 0.1$ and $c_{bl} = 0.025$). As can be seen, within the estimated numerical error, the solution does not depend on α and c_{bl}, *i.e.*, it is grid independent.

Table 3: Pressure foredrag C_{Df}^{p} and its estimated numerical error for several grid clustering and Mach numbers. Euler model.

		C_{Df}^{p}					
α	c_{bl}	$M_\infty = 2$	3	4	5	6	8
2	0.05	0.104 47(3)	0.087 47(5)	0.079 36(4)	0.074 68(3)	0.071 71(2)	0.068 249(8)
1.5	0.05	0.104 47(3)	0.087 47(5)	0.079 36(4)	0.074 68(2)	0.071 71(1)	0.068 252(7)
2.5	0.05	0.104 47(3)	0.087 47(5)	0.079 36(5)	0.074 68(3)	0.071 70(2)	0.068 247(9)
2	0.1	0.104 47(2)	0.087 47(5)	0.079 36(4)	0.074 68(2)	0.071 70(2)	0.068 248(7)
2	0.025	0.104 47(3)	0.087 47(5)	0.079 36(5)	0.074 68(3)	0.071 71(2)	0.068 251(10)

Finally, the pressure foredrag coefficient based on the Euler equations is presented in Tab. 4 together with the solution of the Taylor-Maccoll equation from Sims[12]. The disagreement between Euler solutions and Taylor-Maccoll solution is less than 0.01% for $M_\infty = 2$ and increases with the Mach number, reaching

0.33% for $M_\infty = 8$. The main purpose of this comparison is not quantify the disagreement between the two models, but to show that the obtained solution is in agreement with the solution obtained by another method.

Table 4: Pressure foredrag C_{Df}^p according to Taylor-Maccoll[12] model (TM) and Euler model.

	C_{Df}^p					
Model	$M_\infty = 2$	3	4	5	6	8
TM[12]	0.104 458 29	0.087 475 175	0.079 393 438	0.074 756 914	0.071 828 508	0.068 471 989
Euler	0.104 47(3)	0.087 47(5)	0.079 36(4)	0.074 68(3)	0.071 71(2)	0.068 249(8)

3.2 Navier-Stokes model

3.2.1 Verification

This section deals with the verification of the foredrag coefficient C_{Df} of the Navier-Stokes model. Differently from the Euler model, C_{Df} has two components, the foredrag due to the pressure distribution over the cone surface C_{Df}^p and the foredrag due to the viscous stress C_{Df}^μ, *i.e.*,

$$C_{\mathrm{Df}} = C_{\mathrm{Df}}^p + C_{\mathrm{Df}}^\mu. \tag{12}$$

The input data for the simulations are shown on Tables 5 and 6. Based on these data, simulations were carried on using grids of 60, 120, 240, 480 and 960 volumes in each coordinate direction (grids m_5, m_4, m_3, m_2 and m_1, respectively), where the coarser grids were obtained from the finest one by removing every other grid line.

Table 5: Input data for the Navier-Stokes model.

Quantity	Symbol	Value
Free stream temperature	T_∞	300 K
Length of the elliptical x semi-axis	l_a	0.083 82 m
Length of the elliptical y semi-axis	l_b	0.0508 m
Base radius	r_b	0.0127 m
Fineness ratio (length/base diameter)	f	3
Exponent for boundary nodes distribution	α	2
Multiple of the estimated boundary layer width	c_{bl}	0.04

Table 6: Free stream Mach numbers and the corresponding Reynolds numbers for the Navier-Stokes model.

M_∞	2.73	3.50	4.00	5.05	6.28
Re_∞	2.10×10^6	2.85×10^6	2.16×10^6	1.05×10^6	4.50×10^5

As in the verification of the Euler model, the round-off error here was evaluated for a particular simulation (grid 960×960 and $M_\infty = 2.73$), while the number of iterations were made high enough to reduce the iteration error to the the machine error. It was found that the behavior of the round-off error is similar to that observed in the Euler model. Considering that the round-off and the iteration errors are much smaller than the truncation error, it remains to estimate the discretization error.

The observed order of accuracy calculated for C_{Df}^p and C_{Df}^μ, based on data of the Tables 5 and 6, is shown on Tab. 7. As can be seen, p_U converges to $p_L = 1$ as the grid is refined.

Table 7: Observed order of accuracy of C_{Df}^{p} and C_{Df}^{μ} for the Navier-Stokes model.

	p_U (C_{Df}^{p})					p_U (C_{Df}^{μ})				
Meshes \ M_∞	2.73	3.50	4.00	5.05	6.28	2.73	3.50	4.00	5.05	6.28
(m_3, m_4, m_5)	0.44	0.51	0.56	0.66	0.74	1.57	1.70	1.81	2.15	2.33
(m_2, m_3, m_4)	0.62	0.64	0.68	0.76	0.83	1.27	1.33	1.38	1.54	1.84
(m_1, m_2, m_3)	0.70	0.72	0.77	0.85	0.89	1.13	1.18	1.22	1.30	1.35

Since the solution is in the convergent range, the convergent estimator was applied. Table 8 shows the extrapolated solution and its estimated error. The estimated error of C_{Df} is the sum of the estimated error in C_{Df}^{p} and C_{Df}^{μ} and does not exceed 0.08% of the extrapolated solution. This table also shows the effect of the grid clustering on C_{Df}^{p}, C_{Df}^{μ} and C_{Df} by changing the clustering parameters α and c_{bl}. Within the estimated numerical error, the numerical solution is grid independent.

Table 8: Effect of the grid clustering over C_{Df}^{p}, C_{Df}^{μ} and C_{Df} for some Mach numbers. Navier-Stokes model.

α	c_{bl}	$M_\infty = 2.73$	3.50	4.00	5.05	6.28
				C_{Df}^{p}		
2	0.04	0.083 47(5)	0.076 02(6)	0.072 90(6)	0.068 67(4)	0.066 05(3)
2	0.08	0.083 47(4)	0.076 02(6)	0.072 90(5)	0.068 67(4)	0.066 05(3)
2	0.02	0.083 47(6)	0.076 02(7)	0.072 90(6)	0.068 67(4)	0.066 04(2)
1.5	0.04	0.083 47(5)	0.076 02(6)	0.072 90(5)	0.068 67(3)	0.066 05(2)
2.5	0.04	0.083 47(5)	0.076 02(6)	0.072 90(6)	0.068 67(4)	0.066 05(3)
				C_{Df}^{μ}		
2	0.04	0.005 227(2)	0.004 283(2)	0.004 798(2)	0.006 604(3)	0.009 793(4)
2	0.08	0.005 228(12)	0.004 284(9)	0.004 798(9)	0.006 601(48)	0.009 788(65)
2	0.02	0.005 227(1)	0.004 283(1)	0.004 797(1)	0.006 604(1)	0.009 791(1)
1.5	0.04	0.005 227(2)	0.004 283(2)	0.004 797(2)	0.006 604(3)	0.009 793(4)
2.5	0.04	0.005 227(2)	0.004 283(2)	0.004 798(2)	0.006 604(3)	0.009 793(4)
				C_{Df}		
2	0.04	0.088 70(5)	0.080 30(6)	0.077 70(6)	0.075 28(4)	0.075 84(3)
2	0.08	0.088 70(5)	0.080 30(6)	0.077 70(6)	0.075 27(8)	0.075 84(10)
2	0.02	0.088 70(6)	0.080 30(7)	0.077 70(6)	0.075 28(4)	0.075 83(2)
1.5	0.04	0.088 70(5)	0.080 30(6)	0.077 70(6)	0.075 28(4)	0.075 84(3)
2.5	0.04	0.088 70(5)	0.080 30(7)	0.077 70(6)	0.075 28(4)	0.075 84(3)

3.2.2 Validation

The validation of the foredrag coefficient was performed comparing the results obtained from the Navier-Stokes model and the experimental data of Eggers *et al.*[3]. The experiment was conducted in the Ames 10-14 inch supersonic wind tunnel. The cone models had base diameter of 1 in and length of 3 in. The foredrag force was obtained subtracting the base force from the total drag force, which was measured with a strain-gage balance. The forces on the base of the models were determined from measured base pressures and from free-stream static pressures.

According to Eggers *et al.*, the accuracy of the foredrag coefficients was affected by uncertainties in the measurements of the following quantities: stagnation pressures, free-stream static pressures, base pressures, and the forces on the models as measured by the strain-gage balance. The authors state that the combined effects of all the sources of error result in probable uncertainties in measured foredrag coefficients that varies from ± 0.001 at the low Mach numbers (2.73) to ± 0.005 at a higher Mach numbers

(6.28). Since this experiment was not designed to be a validation experiment, some informations are not available. As an example, the uncertainty over the stagnation pressure p_0, free-stream static pressure p_∞ and dynamic pressure q_∞ are, respectively, 0.5%, 1.5% and 1.5%, but the values of the quantities were not given. On the other hand, the free-stream Mach e Reynolds number were given (see Tab. 6), but their uncertainties were not. Additionally, neither the free-stream temperature nor the base pressure (and their uncertainties) were given.

Table 9 presents the experimental foredrag coefficient ${C_{\mathrm{Df}}}^{\mathrm{exp}}$ of Eggers *et al.* and its expected experimental uncertainty U^{exp}. Since the data were obtained from a plot, ${C_{\mathrm{Df}}}^{\mathrm{exp}}$ is the average value of several readings. The uncertainty due to the data reading U^{read} was calculated as one standard deviation from the mean value and is also shown in Tab. 9. It should be pointed out that all the values of M_∞ read from the plot are in agreement with their nominal values given by Eggers *et al.*, except 6.28 that was read as 6.13(2).

In this work, the reading uncertainty is added to the experimental one. This additional error, that is, the reading uncertainty, is a problem often found when comparing numerical to experimental data.

Table 9: Experimental foredrag coefficient ${C_{\mathrm{Df}}}^{\mathrm{exp}}$ of Eggers *et al.*[3], its experimental uncertainty U^{exp} and reading uncertainty U^{read}.

M_∞	2.73	3.50	4.00	5.05	6.28
${C_{\mathrm{Df}}}^{\mathrm{exp}}$	0.0884	0.0807	0.0784	0.0757	0.0892
U^{exp}	0.0010	0.0020	0.0030	0.0040	0.0050
U^{read}	0.0014	0.0014	0.0014	0.0014	0.0014

Once the estimated numerical error and the expected experimental uncertainty are known, it remains to calculate the input uncertainty in order to estimate the validation metrics. The main input parameters of the Mach2D are the fineness ratio f, the free-stream temperature T_∞, the free-stream Mach number M_∞ and the free-stream Reynolds number Re_∞. Among these parameters, only the uncertainty of f is supposed to be negligible Neither the uncertainty of T_∞ nor its value are known. So, in order to evaluate the influence of T_∞ on the foredrag coefficient, M_∞ and Re_∞ were fixed and three values of T_∞ were assumed: 200 K, 250 K and 300 K. Table 10 shows the extrapolated foredrag coefficient and its error estimate calculated with the convergent estimator as a function of T_∞. As one can see, within the estimated numerical error, T_∞ does not affect the pressure foredrag C_{Df}^{p} and the total foredrag C_{Df} coefficients, but slightly affects the viscous foredrag coefficient C_{Df}^{μ} by an amount up to 0.2%. Taking into account this result, T_∞ was fixed in 300 K and the effect of its uncertainty over C_{Df} was considered negligible

The uncertainty of M_∞ and Re_∞ are estimated using the following idea. Using the ideal gas state equation, it is possible to express the Mach number and the Reynolds number as functions of the free-stream static pressure p_∞ and dynamic pressure q_∞. Since there is an uncertainty of 1.5% over p_∞ and q_∞, it is assumed that the same uncertainty affects M_∞ and Re_∞.

The effect of the uncertainty of M_∞ and Re_∞ over C_{Df}, *i.e.* U^{input}, was calculated based on Eq. (11). The derivatives were numerically approximated with a central differencing scheme and were calculated using two values for ΔM_∞ and $\Delta\mathrm{Re}_\infty$ in order to ensure that the result does not depend on the step size of the finite difference The numerical solution ${C_{\mathrm{Df}}}^{\mathrm{num}}$, its error estimation U^{num} and the effect of the input uncertainty over the numerical foredrag coefficient U^{input} are presented on Tab. 11.

Finally, Tab. 12 shows the validation metrics E and U^{val} of C_{Df}. As one can see, there is a good agreement between the expected numerical and experimental data for $M_\infty < 6.28$. Taking ${C_{\mathrm{Df}}}^{\mathrm{exp}}$ as reference, the relative difference between ${C_{\mathrm{Df}}}^{\mathrm{num}}$ and ${C_{\mathrm{Df}}}^{\mathrm{exp}}$ is less than 0.88%. However, the uncertainty of this relative difference may be as large as 7.1%. The main source of this uncertainty are U^{exp} and U^{read}. For $M_\infty = 6.28$ there is a clear disagreement between the model and the experiment. The reason for this disagreement was not investigated, but it may be caused by the turbulence that was not considered in

Table 10: Effect of the free-stream temperature over C_{Df}^{p}, C_{Df}^{μ} and C_{Df} for some Mach numbers. Navier-Stokes model.

	$M_\infty = 2.73$	3.50	4.00	5.05	6.28
$T_\infty(K)$			C_{Df}^{p}		
300	0.083 47(5)	0.076 02(6)	0.072 90(6)	0.068 67(4)	0.066 05(3)
250	0.083 47(5)	0.076 02(6)	0.072 91(6)	0.068 68(4)	0.066 05(3)
200	0.083 47(5)	0.076 02(6)	0.072 91(6)	0.068 68(4)	0.066 05(3)
			C_{Df}^{μ}		
300	0.005 227(2)	0.004 283(2)	0.004 798(2)	0.006 604(3)	0.009 793(4)
250	0.005 223(2)	0.004 279(2)	0.004 793(2)	0.006 597(3)	0.009 781(4)
200	0.005 221(2)	0.004 277(2)	0.004 790(2)	0.006 593(3)	0.009 774(4)
			C_{Df}		
300	0.088 70(5)	0.080 30(6)	0.077 70(6)	0.075 28(4)	0.075 84(3)
250	0.088 70(5)	0.080 30(6)	0.077 70(6)	0.075 27(4)	0.075 83(3)
200	0.088 69(5)	0.080 30(6)	0.077 70(6)	0.075 27(4)	0.075 83(3)

Table 11: Numerical foredrag coefficient ${C_{\mathrm{Df}}}^{\mathrm{num}}$, its estimated numerical error U^{num} and input uncertainty U^{input} for some Mach numbers. Navier-Stokes model.

M_∞	2.73	3.50	4.00	5.05	6.28
${C_{\mathrm{Df}}}^{\mathrm{num}}$	0.088 70	0.080 30	0.077 70	0.075 28	0.075 84
U^{num}	0.000 05	0.000 06	0.000 06	0.000 04	0.000 03
U^{input}	0.000 52	0.000 40	0.000 35	0.000 28	0.000 23

the model, for instance, or even by an error in the plot of the experimental data (as mentioned earlier, it was found $M_\infty = 6.13$ instead of 6.28 during data reading).

Table 12: Validation metrics for the foredrag coefficient. Comparison of the Navier-Stokes model with experimental data of Eggers *et al.*[3].

M_∞	2.73	3.50	4.00	5.05	6.28
E	0.0003	-0.0004	-0.0007	-0.0004	-0.0134
U^{val}	0.0025	0.0035	0.0044	0.0054	0.0064
$E/{C_{\mathrm{Df}}}^{\mathrm{exp}}$	0.32%	-0.53%	-0.88%	-0.53%	-15%
$U^{\mathrm{val}}/{C_{\mathrm{Df}}}^{\mathrm{exp}}$	2.8%	4.3%	5.6%	7.1%	7.2%

4 Conclusion

The verification of the foredrag coefficient for both the Euler model and Navier-Stokes model showed that the numerical error was dominated by the truncation error, *i.e.*, the iteration error and the round-off error were negligibly small. For all the Mach numbers considered, the observed order of accuracy, calculated using five grids, converged to the asymptotic one, allowing one to apply the convergent estimator for evaluation of the discretization error. The estimated discretization error does not exceed 0.06% of the extrapolated solution for the Euler model and 0.08% for the Navier-Stokes model. The validation metrics of the foredrag coefficient for the Navier-Stokes model showed a disagreement of up to 0.88% between the numerical and experimental results for $2.73 \leq M_\infty < 6.28$ and 15% for $M_\infty = 6.28$. The reason for the last disagreement was not investigated. The estimated validation uncertainty was, at most, 7.2% for the all Mach numbers considered. The main source of this uncertainty was the uncertainty of the experimental

data and due to the reading of the experimental data from a figure. Although this uncertainty is high in the author's opinion, no better option was found for comparing simulation to experimental data. One hopes that the results present here may help other CFD developers.

References

[1] ASME. Standard for verification and validation in computational fluid dynamics and heat transfer, 2009.

[2] R B Bird, W E Stewart, and E N Lightfoot. *Transport phenomena*. John Wiley & Sons, 2 edition, 2002.

[3] A J Eggers, Jr., M M Resnikoff, and D H Dennis. Bodies of revolution having minimum drag at hypersonic airspeeds. Technical report, NACA, 1956.

[4] J H Ferziger and M Peric. *Computational methods for fluid dynamics*. Springer, 3 edition, 2002.

[5] C H Marchi and C R Maliska. A nonorthogonal finite-volume method for the solution of all speed flows using co-located variables. *Numerical Heat Transfer*, 26(3):293–311, 1994.

[6] C H Marchi and A F C Silva. Unidimensional numerical solution error estimation for convergent apparent order. *Numerical Heat Transfer Part B-Fundamentals*, 42(2):167–188, Aug 2002.

[7] B J McBride, S Gordon, and M A Reno. Coefficients for calculating thermodynamic and transport properties of individual species. NASA Technical Memorandum 4513, NASA, 1993.

[8] C M Pilato, B Collins-Sussman, and B W Fitzpatrick. *Version Control with Subversion*. O'Reilly Media, Sebastopol, CA, 2 edition, 2008.

[9] PJ Roache. Quantification of uncertainty in computational fluid dynamics. *Annual Review of Fluid Mechanics*, 29:123–160, 1997.

[10] CJ Roy. Review of code and solution verification procedures for computational simulation. *Journal of Computational Physics*, 205(1):131–156, May 1 2005. International Symposium on Advances in Computational Heat Transfer, New York, NY, Apr, 2004.

[11] J Seward, N Nethercote, and J Weidendorfer. *Valgrind 3.3 - Advanced Debugging and Profiling for GNU/Linux applications*. Network Theory Ltd, United Kingdom, 2008.

[12] J L Sims. Tables for supersonic flow around right circular cones at zero angle of attack. Technical Report SP-3004, NASA, USA, 1964.

[13] George P Sutton and Oscar Biblarz. *Rocket propulsion elements: an introduction to the engineering of rockets*. John Wiley & Sons, United States, 7 edition, 2001.

[14] J C Tannehill, D A Anderson, and R H Pletcher. *Computational fluid mechanics and heat transfer*. Taylor & Francis, 2 edition, 1997.

[15] J P Van Doormaal and G D Raithby. Enhancements of the SIMPLE method for predicting incompressible fluid flows. *Numerical Heat Transfer*, 7:147–163, 1984.

[16] H K Versteeg and W Malalasekera. *An introduction to computational fluid dynamics: the finite volume method.* Longman Scientific & Technical, Harlow, Essex, England, 1995.